IRIS AperTO

UNIVERSITÀ DEGLI STUDI DI TORINO

AperTO - Archivio Istituzionale Open Access dell'Università di Torino

Quantitative Investigation of MgO Bronsted Basicity: DFT, IR, and Calorimetry Study of Methanol Adsorption

This is the author's manuscript

Original Citation:

Availability:

This version is available http://hdl.handle.net/2318/71019 since

Terms of use:

Open Access

Anyone can freely access the full text of works made available as "Open Access". Works made available under a Creative Commons license can be used according to the terms and conditions of said license. Use of all other works requires consent of the right holder (author or publisher) if not exempted from copyright protection by the applicable law.

(Article begins on next page)

23 April 2024

UNIVERSITÀ DEGLI STUDI DI TORINO

This is an author version of the contribution published on:
Questa è la versione dell'autore dell'opera:
J. Phys. Chem. C2010,114,3008–301610.1021/jp909354p

*Hugo Petitjean,Konstantin Tarasov,Françoise Delbecq,Philippe Sautet,Jean Marc Krafft,Philippe Bazin, Maria Cristina Paganini,Elio Giamello, Michel Che,Hélene Lauron-Pernot,and Guyle`ne Costentin**

The definitive version is available at:
http://pubs.acs.org/journal/jpccck

Quantitative investigation of MgO Brønsted basicity: DFT, IR and calorimetry study of methanol adsorption.

Hugo Petitjean,[ab] *Konstantin Tarasov* [ab] *Françoise Delbecq,*[c] *Philippe Sautet,*[c] *Jean Marc Krafft,*[ab] *Philippe Bazin,*[d] *Maria Cristina Paganini,*[e] *Elio Giamello,*[e] *Michel Che,*[abf] *Hélène Lauron-Pernot,*[ab] *Guylène Costentin,**[ab]

[a] UPMC, University Paris 06, UMR 7197, Laboratoire Réactivité de Surface, F-75005 Paris France.

[b] CNRS, UMR 7197, Laboratoire Réactivité de Surface, F-75005 Paris France.

[c] Université de Lyon, laboratoire de Chimie, CNRS, Ecole Normale Supérieure de Lyon, 46 allée d'Italie, 69364 Lyon Cedex 07, France

[d] Laboratoire de Catalyse et Spectrochimie, UMR 6506, 6 Bd du Maréchal Juin, 14050 Caen Cedex, France

[e] Dipartimento di Chimica IFM, Università di Torino, NIS, Nanostructured Interfaces and Surfaces, Centre of Excellence, via Giuria 7, 10125 Torino, Italy

[f] Institut Universitaire de France

hugo.petitjean@enscm.fr, konstantin.tarasov@enscm.fr, Francoise.Delbecq@ens-lyon.fr, Philippe.Sautet@ens-lyon.fr, jean-marc.krafft@upmc.fr, Philippe.bazin@ensicaen.fr,

mariacristina.paganini@unito.it, elio.giamello@unito.it, helene.pernot@upmc.fr, michel.che@upmc.fr, guylene.costentin@upmc.fr,

* Corresponding author: tel.: +33 1 44 27 60 05, fax: +33 1 44 27 60 33

email: guylene.costentin@upmc.fr

ABSTRACT

The adsorption geometries, energies and vibrational frequencies of methanol on MgO defective surfaces have been calculated by periodic DFT simulations. The results are very comparable with those obtained with water and are also in very good accordance with microcalorimetry and infra red experiments. At low coverage, the dissociation is observed on all defects involving ions in low coordinations. Over and above the coordination number of surface ions, the adsorption energy is strongly governed by the surface topology: dissociation on confined sites gives rise to methoxy groups highly stabilized by bridging 2 or even 3 cations. The occurrence of such very strong sites on MgO powder is confirmed by microcalorimetry. The dissociation ability depends on the methanol coverage because it modifies the surface relaxation and the network of H bonds, resulting, for a given defect, in similar adsorption energies for molecular and dissociated species at high coverage. It explains why there are more strong sites (quantified by microcalorimetry) than dissociating sites (quantified by infra-red).

KEYWORDS

Alcohol, adsorption energy, deprotonation, dissociating site, quantification

MANUSCRIPT TEXT

1. Introduction

In heterogeneous catalysis, the first step of most basic reactions is a deprotonation process. So the surface basicity of the catalysts (*e.g.* oxides) is a Brønsted basicity.[1] Thus, it is not straightforward that the usual characterization of the surface basicity of basic oxides by their interaction with CO_2, which is a Lewis acid, is a relevant method to predict the catalytic behavior in a real basic reaction.[2] Protic molecules likely to dissociate can thus be alternatively used to characterize the thermodynamic Brønsted basicity of surfaces. Among them, besides alkynes (acetylene or alkyl acetylene[3-8]), oxoacids (such as water (pKa=14),[9] methanol (pKa=15),[10-14] ethanol (pKa=15.9)[15] and fluoroalcohols[16]) are particularly interesting because the dissociation of oxoacids is involved in a large class of basic reactions (saponification, transesterification, etherification).[17,18]

Methanol (MeOH), the simplest alcohol, is one of the most widely used protic probe molecule. Its dissociation leads to the formation of hydroxyl and methoxy groups that can be characterized by infra-red spectroscopy. Bensitel et al.[10] have proposed an assignment of the ν_{CO} stretching bands in relation with the molecular/dissociative adsorption modes of MeOH and the coordination number of the methoxy group. This empirical model was already used to classify the deprotonation abilities of MgO samples with various morphologies and allowed us to discuss the relationship between dissociation equilibrium of MeOH and basic reactivity of 2-methylbut-3-yn-2-ol.[13,19]

The aim of the present paper is to establish methanol adsorption as a quantitative tool to investigate surface basicity on a model inorganic basic oxide, MgO. Quantitative data on the strength and the number of sites involved in the deprotonation process are discussed in relation with their nature. DFT modeling can help to explicitly connect the adsorption energies with the adsorption modes of the probe and the nature of the involved MgO pair. Modeling of the various $Mg_{LC}^{2+}O_{L'C}^{2-}$ pairs existing on defective MgO surfaces (LC and L'C stand for the coordination numbers of magnesium cation and oxide anion, respectively) (see figure S1-1) has already been validated.[20-24] These structure models are

used here to calculate adsorption structures of methanol (adsorption geometries and energies) as well as vibrational frequencies depending on the localization of the adsorption site and on the methanol coverage. Results from calculations are discussed in relation with experimental data. Infra-red is the best tool to investigate the adsorption modes of a molecule on a surface and may also provide interesting information on the strength of interaction of a surface with probe molecules from frequency shift measurements. Thermo-desorption measurements may also provide useful data on the strength of interaction, but it is not appropriate in the case of methanol, since methanol molecule can react upon thermo-desorption, with dehydrogenation of the molecule above 573 K. Thus, even though there are very few literature dealing with alcohol adsorption followed by microcalorimetry,[25-27] this technique appears to be the most suitable to experimentally study the strength of interaction of methanol with MgO surface. Since both infra-red and microcalorimetry techniques were performed within the same experimental protocol, energy values deduced from microcalorimetry will be accurately discussed in relation with adsorption modes followed by infra-red. As the absorption coefficients related to ν_{CO} vibration modes of methanol adsorbed on MgO powders are available,[28] the absolute amounts of sites can be measured with the two techniques and will be compared.

2. Experimental and computational section

2.1 Computational methods

2.1.1 Methods

The periodic calculations are performed in the framework of the density functional theory (DFT) and the generalized gradient approximation exchange-correlation functional of Perdew and Wang PW91,[29] as implemented in the Vienna Ab Initio Simulation Package (VASP 4.6).[30,31] The one electron wave function is developed on a basis set of plane waves and the interaction between the core and the valence electrons is described by the projector augmented waves (PAW) approach.[32] From preliminary studies on water, its dimer and methanol (results not shown), PAW core radius of 1.52 Å for oxygen and 1.50 Å for carbon and an energy cutoff value of 400 eV were chosen since larger radius (and lower

cutoff) overestimate covalent bond lengths and underestimate hydrogen-bond length too drastically.[23] The convergence criterion for the electronic self-consistent cycle has been fixed to 10^{-6} eV per cell. Geometry optimizations are performed within a conjugate-gradient algorithm until the convergence criterion on forces (10^{-2} eV.Å^{-1}) is reached. The slabs are not symmetrical, which induces a net dipole and consequently a spurious electrostatic interaction between the slab and its periodic images along the z axis. A dipolar correction along the perpendicular to the slab has been applied to remove this effect. This correction does not exceed 0.05 ‰ of the total cohesive energy.

The average adsorption energy per methanol molecule is calculated at 0 K thanks to equation 1, where U_{relax}^{ads}, U_{relax}^{bare}, $U_{methanol}$ are the energies of the relaxed system with adsorbed methanol, of the relaxed bare system and of the methanol molecule, respectively. n_{ads} stands for the number of methanol molecules per supercell.

$$\Delta_{ads}U_{(0K)} = \frac{1}{n_{ads}}(U_{relax(0K)}^{ads} - U_{relax(0K)}^{bare} - n_{ads}U_{methanol(0K)}) \qquad \text{Eq. (1)}$$

The adsorption energy per additional methanol molecule adsorbed at 0K on system already adsorbing n_{ads} molecule is given by equation 2 where $U_{relax(0K)}^{(n_{ads}+1)}$, $U_{relax(0K)}^{n_{ads}}$ are the energies of the relaxed system with (n_{ads}+1) and n_{ads} adsorbed methanol molecules, respectively.

$$\Delta_{ads}U_{(0K)}^{n_{ads}} = U_{relax(0K)}^{(n_{ads}+1)} - U_{relax(0K)}^{n_{ads}} - U_{methanol(0K)} \qquad \text{Eq. (2)}$$

The vibrational frequencies of adsorbed methanol on MgO systems are calculated numerically, with a displacement of ±0.02 Å around the equilibrium position. Preliminary calculations have shown that the coupling with the surface modes cannot be totally neglected, so magnesium and oxygen surface atoms in direct interaction with methanol were allowed to move, in addition to methanol atoms.

Isolated methanol molecule in gas phase is used as a reference in order to estimate the systematic deviation between experimental[33] and calculated ν_{CO} values. The obtained scale factor includes implicit corrections related to the calculation method and anharmonicity corrections that were not separately calculated considering that they are quite low in the ν_{CO} range (~1000-1200 cm^{-1}).

2.1.2. Systems

2.1.2.1. MgO surfaces.

MgO surface irregularities with 3C and 4C ions (figure S1-1) were described in a previous work with a slab approach using periodic boundary conditions.[20] The systems modeling these irregularities, including in their hydroxylated form resulted from water dissociation, were shown to be representative of real surfaces.[20,23] In addition to these defective systems, 5C ions are also considered here. They are modeled by the terrace system T. 4C ions are described by monoatomic steps (terraces size: three times d_{Mg-O}, called S1) and diatomic steps (terraces size: $2d_{Mg-O}$, called S2). The T, S1 and S2 slabs are composed of 3 layers of ions, which was proved to provide a converged description of the electronic structure for MgO (100).[34] 3C ions are modeled by the corner systems C3 with length of the edge between $O^{2-}{}_{3C}$ and $Mg^{2+}{}_{3C}$ of $3d_{Mg-O}$ (this was shown to be large enough to model at the same time $Mg^{2+}{}_{3C}$ (C3-Mg_{3C}) and $O^{2-}{}_{3C}$ (C3-O_{3C}) terminated corners[20]). 3C ions in a more confined environment are modeled by a divacancy, referred to as D, which is performed in the edge of S1, and by kinks, called K, also performed on S1 by formally removing 4 atoms in its edge. Characteristics of the various systems are summarized in table 1.

For S1, S2, D and K, the lowest layer of ions is constrained at the bulk geometry, whereas the other ones are allowed to relax. For the bigger C3 model, the first and second neighbors of surface ions on the edge between the $O^{2-}{}_{3C}$ and the $Mg^{2+}{}_{3C}$ are relaxed.

Table 1: Systems and parameters used for the simulation of MgO surface defects

System	5C	4C		3C		
	Terrace T	Steps S1	S2	Corner C3	Divacancy D	Kink K
Number of atoms	48	72	72	156	88	116
Dimension (Å) along the :						
x-axis	8.51	6.73	6.02	6.73	9.02	9.,02
y- axis	8.51	12.76	12.76	17.01	12.76	17.01
number of MgOpair on the along y-axis	2	3	3	4	3	4
z-axis vacuum thickness	16.5	16.5	16.5	16.5	16.5	16.5
slab thickness	4.25	7.44	9.02	15.04	9.92	9.92
projected surface areas A (Å²)	72.38	85.83	76.77	153.53	85.83	114.44
k point mesh	2x2x1	2x1x1	2x1x1	2x1x1	2x1x1	2x1x1

2.1.2.2. Methanol adsorption

Adsorption at the edge of the steps (S1 and S2-ON where ON means "on" the edge) (figure S1-1) is performed at various methanol coverages. The related systems with several adsorbed methanol molecules are named as follows: "system-n_{ads}m", where n_{ads} stands for the number of methanol molecules per unit cell. Only the adsorption of a single molecule is studied for other systems (n_{ads}=1 for corners, kinks and divacancies). Carbon, oxygen and hydrogen atoms coming from methanol are relaxed, in addition to the ions relaxed in bare surface models. For a given defect, adsorption structure is optimized starting from molecular methanol in weak interaction with surface ions to test non-dissociative adsorption. "system-H-1m" labeling is used for adsorption structures resulting from simple H-bonding between methanol molecule and surface O^{2-}_{LC}.

When dissociation is effective, an adsorbed methoxy on a Mg^{2+}_{LC} and a hydroxyl $O_{LC}H$ are obtained. From this point, several stable situations are conceivable, depending on whether the two groups are next to each other or not. In this work, only the most exothermic case is explored, according to the stabilization rules obtained from previous work on hydration.[20] Most of the time, it comes down to prefer a structure with H-bonding between adsorbed methoxy and hydroxyl (see details in S2 section).

2.2 Sample preparation

$Mg(OH)_2$ precursor of MgO was obtained by sol-gel method from magnesium methanolate (Mg: Aldrich, 99.5 %; methanol: Acros Organics, H_2O < 0.005). This precursor was then decomposed in vacuum (10^{-3} Torr) (1Torr = 133,32 Pa) up to 1273 K (ramp 1 $K.min^{-1}$), kept at this temperature for 2 h and further treated under static oxygen (10 Torr) at 673 K for 30 min to remove the organic surface residues. The periclase structure of the obtained sample was checked by XRD and its specific surface area value, evaluated by the BET method, was 150 $m^2.g^{-1}$.

2.3 Microcalorimetry

The microcalorimetric studies of methanol adsorption on MgO sol gel were performed at 303 K in a heat flow Tian-Calvet microcalorimeter (Setaram, France) connected to a volumetric apparatus, which enabled the simultaneous determination of adsorbed amounts, released heat**,** and equilibrium pressure for small increments of the adsorptive probe.[35] Methanol (Prolabo, RP Normapur) was

previously purified using freeze-pump-thaw cycles. Before any adsorption, 100 mg of sample was outgassed in quartz ampoules at 1173 K for one hour in dynamic vacuum and the tightly closed ampoules were then transferred into the microcalorimetric setup. In order to measure the integrated heat of adsorption as a function of coverage, small doses of methanol were repeatedly let in onto the catalyst until the measured value corresponds to the heat of condensation of methanol (-35kJ.mol^{-1}).[36] Desorption step was gradually performed and the sample was finally outgassed under secondary vacuum (7.5 10^{-7} Torr). A second adsorption was performed in order to quantify the amount of methanol irreversibly chemisorbed at this pressure.

2.4 FTIR

A self-supported wafer of about 20–30 mg was placed in an *in situ* quartz cell, designed and homemade to reach 1173 K. The sample was pretreated following the procedure described in ref. 13 up to 1173 K for one hour under vacuum. Then, the wafer was brought from the furnace part of the cell to the optical one (fitted out with ZnSe windows), at RT. All spectra were thus registered at room temperature using a Bruker FTIR Vector 22 spectrometer, fitted out with a DTGS detector (resolution 2 cm^{-1}, 128 scans/spectrum). Methanol (Prolabo, RP Normapur, further purified by freeze-pump-thaw), was contacted with MgO by successive doses at room temperature via a vacuum line connected to the spectrometer. A final equilibrium pressure of 1 Torr was obtained after 15 min of contact with the sample. The IR spectrum of the gas phase and of the bare wafer were recorded and subtracted from the spectrum of the wafer covered with methanol. Afterwards, the 1000-1200 cm^{-1} domain was decomposed in several Gaussian curves with Levenberg-Marquardt algorithm implemented in ORIGIN 6.1. The minimization of the x2-value was always found above 0.999. Quantification of the dissociative and molecular contributions of methanol adsorbed was achieved thanks to prior determination of the absorption coefficients: all contributions related to dissociation have the same absorption coefficient, 6.2 cm.µmol^{-1} whereas that corresponding to molecular adsorption mode was found to be 2.5 cm.µmol^{-1}.[28]

3. Results and Discussion

3.1 Geometries of methanol adsorbed on MgO systems.

3.1.1 Low coverage

At low methanol coverage (n_{ads}=1), corresponding to the adsorption of one molecule per cell, dissociation of methanol is observed for all the systems, except for terraces T for which two stable structures are found (figure 1). In the first structure, T-1m, methanol interacts with Mg^{2+}_{5C} cation and O^{2-}_{5C} anion via its oxygen atoms and via H-bond donor interaction respectively. In the second one, T-H-1m, a simple H-bond interaction between the OH group of the molecule and O^{2-}_{5C} surface anion.

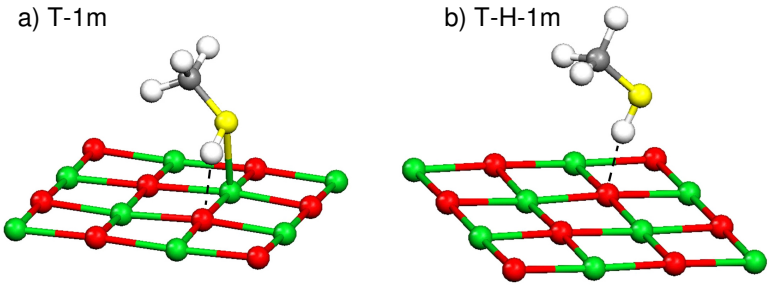

Figure 1: Outmost layer of the (100) terrace with one methanol molecule adsorbed. a) T-1m structure: interaction between OH group of methanol and an $Mg^{2+}_{5C}O^{2-}_{5C}$ pair, b) T-H-1m structure: H-bonding interaction between O^{2-}_{5C} and proton of the OH group. H, C, O atoms of methanol are represented in white, grey and yellow, whereas Mg and O surface atoms are green and red, respectively.

Stable dissociative adsorption is systematically observed for all other systems. An additional stable molecular adsorption is evidenced only in the case of C3-O_{3C} system: it results from the H bond interaction between hydroxyl group of methanol and surface O^{2-}_{3C} with d(H-O^{2-}_{3C}) = 1,600 Å. Consistently with the increase of electronic density on O^{2-}_{3C} compared to O^{2-}_{5C}, this H bond length is shortened by 5% compared to that involved in T-H-1m.

Dissociative adsorptions result from deprotonation of methanol. The proton H^+ and $O_{L"}Me^-$ methoxy fragments adsorb on $O^{2-}_{L'C}$ anion and Mg^{2+}_{LC} cation(s) respectively (L" being the coordination number of the oxygen atom of the methoxy group). The two fragments interact via H bonding, except in D-1m and K-1m . A monocoordinated methoxy $O_{1C}Me^-$ (its oxygen atom is coordinated with only one magnesium cation) is only observed in the case of the C3 and S2-ON convex systems (figure 2 a). As already observed in the case of dissociative adsorption of water on MgO systems,[20] bridging involving

several Mg^{2+} cations occurs for concave systems: it results in O_{2C}Me groups for S1 and S2-IN and in O_{3C}Me groups for K and D (figure 2b). Note that the latter configuration has never been reported before for alcohol adsorption on MgO. Moreover, the geometric parameters obtained are also very similar with those observed in the case of water adsorption (S3 and table S3-1).

3.1.2 Influence of the coverage

The influence of the methanol coverage is evaluated on edges of steps (S1 and S2-ON systems), adsorbing two or three methanol molecules (n_{ads}= 2 or 3 corresponding to θ = 66 or 100%, respectively). Stable adsorption structures are obtained and the qualitative trends are the same than those observed at low coverage: methanol dissociates and forms, mono- and di-coordinated methoxy groups for S2-ON and S1, respectively. The methoxy groups are H-bonded with the vicinal hydroxyls. However, in the case of S2-ON-3m, two stable structures are obtained, S2-ON-3m-*fd* and S2-ON-3m-*pd*, where full dissociation (*fd*) and partial dissociation (*pd*) are observed respectively. In the latter case, one molecule out of three is not dissociated (figure 3). In fact, the higher the coverage, the lower the relaxation ability of the surface (table S3-1): d(Mg^{2+}_{LC}-O^{2-}_{LC}) distances decrease upon adsorption of the second and the third molecules and, finally, d(Mg^{2+}_{LC}-O^{2-}_{LC}) distances in the S1-3m and S2-ON-3m systems are only 6% longer than in the corresponding bare systems (2.13 Å). As already mentioned in the case of water adsorption,[20] this phenomenon proceeds from simple mechanical constraints. When the first molecule is adsorbing, the related d(Mg^{2+}_{LC}-O^{2-}_{LC}) distance is increasing of 31%. An equivalent surface relaxation upon further adsorption on two neighboring $Mg^{2+}_{LC}O^{2-}_{LC}$ pairs would result in a too important shortening between the two pairs.

H bonding interactions are also modified upon methanol coverage. The d($O_{methoxy}$-H) distance corresponding to H-bond increases with methanol coverage for S1 (from 1.89 to ~2.03 Å) whereas it decreases for S2-ON (from 1.43 Å for S2-ON-1m to 1.35 Å in the case of S2-ON-3m-*fd*). The increase of methanol coverage therefore tends to increase the dissociation for S1, but to decrease it in the case of S2-ON, to such a point that it results in mixed molecular and dissociative adsorption modes on the latter system for θ = 1 (S2-ON-3m-*pd*) (table S3-1).

Figure 2: Methanol dissociative adsorption structures involving a) O_{1C}-Me monocoordinated methoxy group for convex C3 corners and S2-ON edge of step systems (L"=1), b) $O_{L",C}$-Me multicoordinated methoxy group for concave S1-1m monoatomic step, S2-IN-1m valley (L"=2) and K-1m kink, D-1m divacancy (L"=3). No H bond interaction is observed when L"=3. H, C, O atoms of methanol are represented in white, grey and yellow, whereas Mg and O surface atoms are green and red, respectively.

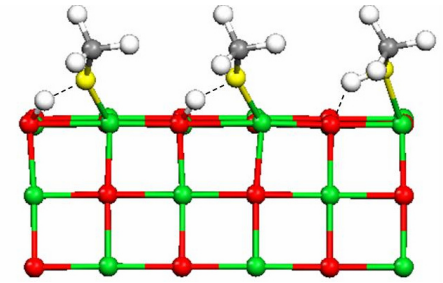

Figure 3 : S2-ON-3m-*pd* structure corresponding to the full methanol adsorption on the edge of high steps, S2-ON, showing that one out of three methanol molecule ("3m") is not dissociated (*pd* stands for partial dissociation).

3.2 Description of Adsorption modes by infra-red spectroscopy

The adsorption modes of methanol on MgO surface defects can be characterized thanks to infra-

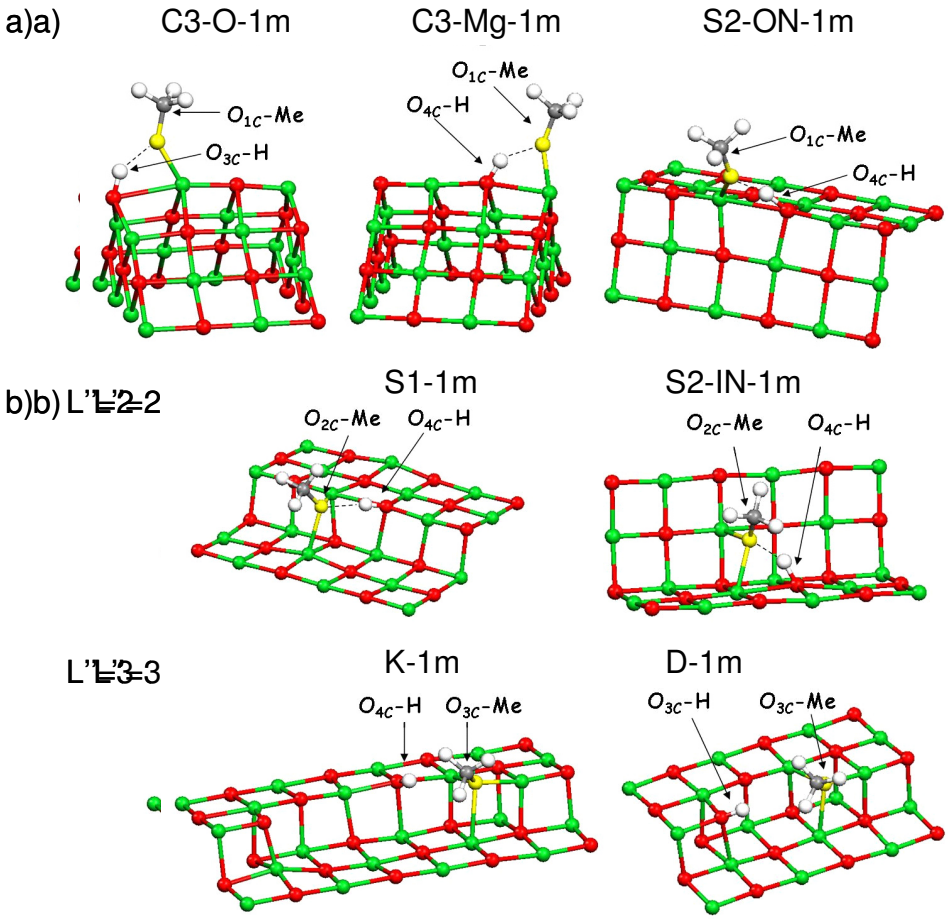

red spectroscopy. The assignment of experimental spectra proposed by Bensitel et al. was based on the use of MgO of various morphologies, on the adsorption of labeled molecules and on the analogy with infra-red data related to methanol adsorbed on other oxides.[10] It does not take into account the occurrence of tri coordinated methoxy groups evidenced in the previous section although such contribution was mentioned in the case of methanol adsorption on ceria[33] or ceria-zirconia[37]. DFT calculations of vibrational frequencies have thus been undertaken to check and precise the former assignments.

Systems representative of the various adsorption modes described above are considered. T-1m and T-H-1m represent molecular mode. Dissociative modes are represented with concave areas (S1-1m, S2-IN-1m and D-1m) and with convex areas (S2-ON-1m and C3-Mg-1m). Note that these systems include adsorption sites of various coordination numbers and involve the coordination of 1, 2 and 3 magnesium cations by a methoxy group. In addition, the influence of lateral interactions occurring at high coverage is considered in the case of S2-ON-3m-*fd* and S2-ON-3m-*pd*, for fully dissociative and mixed adsorption modes respectively.

The calculated harmonic frequencies related to the various vibrational modes of methanol adsorbed on the various defects are gathered in table S4-1. Among them, the stretching vibration related to the C-O bond that corresponds to quite intense vibrations in the 1000-1150 cm^{-1} range, is usually considered as the most accurate to follow methanol adsorption. This is confirmed by the detailed analysis of table S4-1 reported in S4. The calculated values of the ν_{CO} frequencies, ordered in relation with the type of adsorption mode involved, are reported in table 2.

The harmonic calculation of frequencies related to gaseous methanol leads to two ν_{CO} contributions at 1009 and 1055 cm^{-1} related to stretching vibrations coupled with δ_{OH} and ρ_{CH3} modes. In the experimental data, only one mode is active. From a calculation of intensities[38] we showed that the low frequency component is 25 times more active than the high frequency one. The experimental band at 1032 cm^{-1} is thus related to that calculated with VASP at 1009 cm^{-1}, the ratio between these two frequencies, 1.023 was used as scale factor to get corrected calculated ν_{CO} frequencies to be compared to

experimental data. This ratio takes into account several approximations in the calculations (DFT functional, harmonic approximation, …).

The comparison of the calculated values scaled by the above factor with the experimental ones that are reported in table 2 shows that they are in good agreement, although the former are systematically overestimated. The adsorption mode appears as a deciding parameter governing the ν_{CO} stretching frequency. The calculated frequencies can be gathered within four groups i) molecular adsorption at 1065±2 cm^{-1}, ii) dissociative with L"=1 at 1152±11 cm^{-1}, iii) dissociative with L"=2 at 1105 cm^{-1}, but also iv) dissociative resulting in a methoxy group with L"=3 at 1086 cm^{-1}. The three first groups are in very good accordance with the assignment proposed by Bensitel et al.,[10] molecular adsorption, type I and II dissociative adsorptions, respectively. Furthermore, the present work takes into account a new contribution related to the existence of tri-coordinated methoxy group evidenced in section 3.1.1, but never considered in previous infra-red studies.

The frequency range is quite narrow inside each group. The molecular/dissociative nature of the adsorption mode is the main parameter governing the ν_{CO} frequency: the molecular adsorption mode is shifted of only 23 cm^{-1} compared to the gas phase, whereas all the dissociative modes are more strongly shifted (from 54 to 131 cm^{-1}). Among the molecular adsorption modes, there is almost no influence of the electronic donation of the oxygen of MeOH toward the surface (shift of only 3 cm^{-1} between T-1m and T-H-1m). In the case of dissociative adsorption modes, this electronic donation effect is much more pronounced and is promoted by increasing the number of magnesium cations in interaction with methoxy species (L" value). Thus, the higher the L" value, the lower the electronic density of the C-O bond, the weaker the C-O bond, the lower the wavenumber of the related vibrator. As the coordination number L" of the oxygen of the methoxy group is directly related to the surface topology, this feature appears much more important than the coordination number of the adsorption site itself. Indeed, the methoxy species (L"=2) formed on S2-IN-1m and bridging two Mg^{2+}_{5C} leads to the same frequency than the one formed on S1-1m bridging one Mg^{2+}_{5C} and one Mg^{2+}_{4C}. However, the coordination number of the adsorption sites may act as a second order parameter. For example, among monocoordinated

methoxy species (L"=1), the slight decrease of the ν_{CO} observed from S2-ON to C3-Mg_{3C}-1m (1157 to 1141 cm^{-1}) is consistent with the decreasing coordination number of the magnesium cation Mg^{2+}_{4C} versus Mg^{2+}_{3C}: when the unsaturation of the bare cation is increased, the delocalisation of the electronic density of the C-O bond on the cation is enhanced.

Table 2: Calculated ν_{CO} harmonic frequencies related to isolated methanol molecule and to adsorbed methanol molecule on MgO defects. Comparison of the corrected calculated $\nu_{CO\ corr}$ values with experimental $\nu_{CO\ exp}$ data and related assignment is also presented. For the system S2-ON-3m-*pd*, data reported correspond to the molecularly adsorbed molecule.

system	Ions involved	calculated ν_{CO}	$\nu_{CO\ corr}$ (cm^{-1})*	$\nu_{CO\ exp}$ (cm^{-1})	Adsorption mode
Isolated methanol		1009 ($+\rho_{CH3}$)	1032	1032	-
T-1m	Mg^{2+}_{5C} O^{2-}_{5C}	1040	1064	1060	Molecular
T-H-1m	O^{2-}_{5C}	1043	1067		
S2-ON-3m-*pd*	Mg^{2+}_{4C} O^{2-}_{4C}	1043	1067		
S2-ON-1m	Mg^{2+}_{4C} O^{2-}_{4C}	1131	1157	1115	dissociative L"=1
S2-ON-3m-*fd*	Mg^{2+}_{4C} O^{2-}_{4C}	1137	1163		
C3-1m-Mg_{3C}	Mg^{2+}_{3C} O^{2-}_{4C}	1116	1141		
S1-1m	Mg^{2+}_{4C} Mg^{2+}_{5C} O^{2-}_{4C}	1080	1105	1092	dissociative L"=2
S2-IN-1m	Mg^{2+}_{5C} Mg^{2+}_{5C} O^{2-}_{4C}	1080	1105		
D-1m	Mg^{2+}_{3C} Mg^{2+}_{4C} Mg^{2+}_{5C} O^{2-}_{4C}	1062	1086	Not reported	dissociative L"=3

* $\nu_{CO\ corr.} = (1032/1009) \times \nu_{CO\ calc.} = 1.023 \times \nu_{CO\ calc.}$

3.3 Adsorption energies of methanol adsorbed on MgO systems

3.3.1 Calculated energies

In any cases, the MgO surface is stabilized upon methanol adsorption, as shown by the negative values calculated for adsorption energies $\Delta_{ads}U_{(0K)}$ (eq.1) reported in table 3 that are ranging from -32 to -372 kJ.mol^{-1} At low coverage, molecular adsorption leads to a weaker interaction than the dissociative one as evidenced by comparing the more stabilizing molecular system (C3-O_{3C}-H-1m) with the less stabilizing dissociative one (S2-IN) (-63 and -88 kJ.mol^{-1}, respectively) or the two adsorption modes for the same system, C3-O_{3C}-H-1m and C3-O_{3C}-1m (-63 and -156 kJ.mol^{-1}, respectively).

Opposite to results obtained by Branda et al. who only considered non relaxed clusters,[39] the molecular adsorption by simple H bonding (T-H-1m) between surface oxygen and proton of the methanol molecule is also found less stabilizing than that involving interaction between oxygen of the methanol and surface magnesium (T-1m). However, the stabilization observed for C3-H-1m-O_{3C} system is much higher than that of T-1m, indicating that the coordination number of the $O^{2-}{}_{LC}$ anion which is H-bond acceptor (L'=3 and 5, respectively) influences the adsorption strength.

The stabilization increases for dissociative adsorption following S2-IN-1m < S2-ON-1m < C3-Mg_{3C}-1m < C3-O_{3C}-1m < S1-1m < K< D, which is exactly the order previously found in case of water.[20] Moreover, the energy stabilization is very comparable for both molecules, being exactly the same (372 kJ.mol^{-1}) for D. In fact, stability is governed at first order by the topology of the site with overstabilization on concave areas compared to convex ones (see for instance S1-1m [L"=2] that involves a bridging adsorption simultaneously on a 4C and a 5C ions [-181 kJ.mol^{-1}] compared to C3-1m [L"=1] that involves a single Mg ion in lower coordination, 3C or 4 C [-140,-156 kJ.mol^{-1}]). The second order and weaker influence is from the coordination numbers L and L' of the adsorbing $Mg^{2+}{}_{LC}O^{2-}{}_{L'C}$ pair (see among convex areas C3-1m-Mg_{3C} with L=3 and L'=4 [-140 kJ.mol^{-1}] and S2-ON-1m with L=4 and L'=4 [-129 kJ.mol^{-1}]).

It can also be seen from table 4 that, for a given considered system (S1 or S2-ON), increasing the coverage results in a relative decrease of the average stabilization per methanol adsorbed. This trend is confirmed by calculating the adsorption energy $\Delta_{ads}U^{nads}{}_{(0K)}$ per additional adsorption of one methanol molecule (eq.2) on a system previously adsorbing n_{ads} molecules. Indeed, from table 4, adsorbing the

second molecule on S1 and S2-ON systems (up to a 2/3 coverage) is less stabilizing than the first one by 40 $kJ.mol^{-1}$. This is mainly due to the constraints between the deformations generated by each adsorbate on the MgO surface, which are not compatible at high coverage (see section 3.1.2). Note however that the adsorption energy is not further decreased for the third molecule (coverage 1), with roughly the same differential adsorption energy than the second one. Surprisingly, in the case of S1, whereas the adsorbates are less stabilized at high coverage than at low coverage, they are more dissociated (the distance between proton and methoxy group is increased). Since the H bonding between the two dissociated moieties plays a part in stabilizing the adsorbate, a site with lower strength is not necessarily less dissociating. In the same way, from comparison of S2-ON-3m-*pd* and S2-ON-3m-*fd* systems, the adsorption of a third molecule in its molecular form is comparatively slightly more exothermic than in the dissociated form. This is consistent with the decreasing dissociation ability upon increasing methanol coverage described above: as the constraints at high coverage prevent the two moieties $O_{4C}H$ and $O_{1C}Me$ from effective H-bonding, the recombination into adsorbed molecular methanol is favored. Contrary to what is usually intuitively considered, there is thus no direct relationship between dissociation level and stabilization level of the adsorbed structure: the dissociation ability is effectively related to the nature of the site, but is also greatly influenced by the methanol coverage.

Table 3: Adsorption energies $\Delta_{ads}U$ (kJ.mol^{-1}) per methanol molecule for the surface defects modeled for MgO

Surface sites	**Terrace T**		**Step S2-IN**	**Step S1**	**Step S2-ON**	**Corner C3-**			**Divacancy D**	**Kink K**
Ions involved	Mg^{2+}_{5C}, O^{2-}_{5C}		Mg^{2+}_{5C}, Mg^{2+}_{5C}, O^{2-}_{5C}	Mg^{2+}_{4C}, Mg^{2+}_{5C}, O^{2-}_{4C}	Mg^{2+}_{4C}, O^{2-}_{4C}	O^{2-}_{3C}	Mg^{2+}_{4C}, O^{2-}_{3C}	Mg^{2+}_{3C}, O^{2-}_{4C}	Mg^{2+}_{3C},Mg^{2+}_{4C}, Mg^{2+}_{5C}, O^{2-}_{3C}	Mg^{2+}_{3C}, Mg^{2+}_{4C}, Mg^{2+}_{5C}, O^{2-}_{4C}
systems	***T-H-1m****	***T-1m****	***S2-IN-1m***	***S1-1m***	***S2-ON-1m***	***C3-H-1m-O_{3C}****	***C3-1m-O_{3C}***	***C3-1m-Mg_{3C}***	***D-1m-Mg_{3C}-O_{3C}***	***K-1m-Mg_{3C}-O_{4C}***
$\Delta_{ads}U$	-32	-49	-88	-181	-129	-63	-156	-140	-372	-242

* molecular adsorption

Table 4: Influence of methanol coverage on the average adsorption energies $\Delta_{ads}U$ and adsorption energies $\Delta_{ads}U^{n_{ads}}_{(0K)}$ per additional methanol molecule adsorbed on S1 and S2-ON systems

	$\Delta_{ads}U$				$\Delta_{ads}U^{n_{ads}}_{(0K)}$			
	S-1m	S-2m	S-3m-*fd*	S-3m-*pd*	S → S-1m	S-1m → S-2m	S-2m → S-3m-*fd*	S-2m → S-3m-*pd*
S1	-181	-161	-156		-181	-141	-146	-
S2-ON	-129	-106	-98	-101	-129	-84	-81	-89

3.3.2 Microcalorimetry

The surface basicity in terms of strength and number of basic sites (leading to irreversible chemisorption of methanol) was determined by methanol adsorption followed by microcalorimetry. Figure 4 represents the experimental differential molar adsorption heats measured at 303 K as a function of the amount of methanol adsorbed during the first incremental adsorption step. Adsorption energies calculated at 0K at low coverage (n_{ads}=1) for the various systems are reported for comparison. Taking into account that the expected error between experimental data obtained at 303 K and calculated ones at 0K was estimated to 7.5 kJ.mol^{-1}, ($\Delta_{ads}U_{(303K)}$ - $\Delta_{ads}U_{(0K)}$ = $\int_{T=0K}^{T=303K} C_v.dT$ = 7.5 kJ.mol^{-1}, where C_v, the calorific capacity at constant volume of methanol gas, is considered as a constant (25J.mol^{-1}.K^{-1} at 303 K), the experimental data range is in very good agreement with that of calculated values.

Moreover, the microcalorimetry provides an experimental proof for the existence of the adsorbed structures involving tricoordinated methoxy groups ascribed to methanol adsorbed on divacancies and kinks. Their calculated adsorption energies (-372 and -242 kJ.mol^{-1}, respectively) are very consistent with the strongest measured energy value, about 300 kJ.mol^{-1}, which is in fact an average value for the first methanol dose adsorbed on the strongest sites.

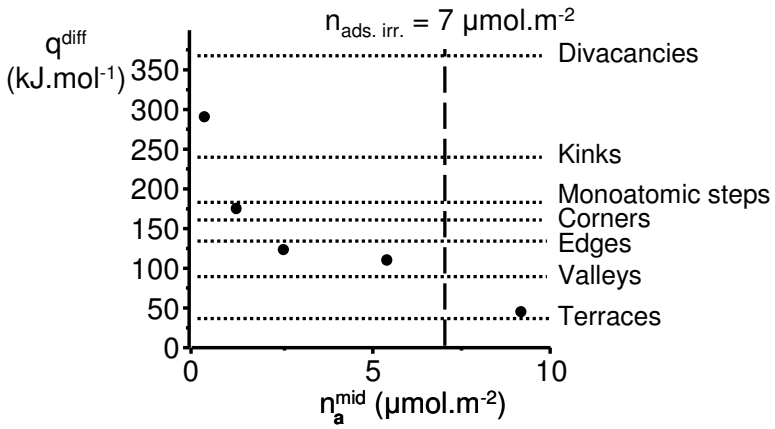

Figure 4 : Experimental differential molar adsorption heat q^{diff} as a function of n_a^{mid}, $n_a^{mid} = n_a^{prev} + \frac{\Delta n_a}{2}$ where n_a^{prev} is the amount of methanol already adsorbed at the previous point and Δn_a is the amount of additional molecules. Calculated adsorption energies on Divacancies (D-1m), Kinks (K-1m), Monoatomic steps (S1-1m), Corners (C3-1m-O3C), edges (S2-

ON-1m), valleys (S2-IN-1m) and terraces (T-H-1m) for low coverage (n_{ads}=1) , are indicated by the horizontal dotted lines. The vertical dashed line shows the limit amount corresponding to irreversible adsorption (see text).

3.4 Quantification of the sites: irreversible adsorption versus adsorption modes

According to the microcalorimetry data, during primary adsorption (figure 4), methanol (~1µmol.m^{-2}) first interacts with the strongest sites (q^{diff}> 150 kJ.mol^{-1}), the next 2-5 µmol.m^{-2} adsorb on middle strength sites in the 150-100 kJ.mol^{-1} range and then the last doses adsorb on the weakest sites (~50 kJ.mol^{-1}). Considering the exposed area by one Mg-O pair, assimilated to the one on (100) ideal plane 8.87 10^{-20} m^2, and cell parameter of 2.1065 Å,[41] the strongest and middle strength sites are roughly estimated to correspond to around 5 and 25% of the total exposed surface of the sample, respectively. The amount of irreversibly adsorbed methanol molecules can be more accurately estimated from the comparison of primary and secondary adsorption steps: its value can be deduced from the x-axis shift required to overlay the two curves representing $Q_{tot}=f(n_{asd})$ (figure not shown) for the two adsorptions and was estimated to be 7 µmol.m^{-2}, which corresponds to about 35% of total exposed surface.

This value was reported on the figure 4, in order to determine the nature of the sites involved in such irreversible adsorption. However, the related limit q^{diff} value ranges from 110 to 50 kJ.mol^{-1} due to too large incremental methanol doses. Moreover, this q^{diff} value is an average value of the heat of adsorption measured for a large incremental MeOH dose, so it could possibly involve various sites. Complementary insight can be deduced from the calculation of the differential adsorption heat that is given (in kJ.mol^{-1}) by equation 4. (see S6)

$$q_{diff}(n_a) = -RT + TS°_{méthanol}(T) - RT\ln\left(\frac{p}{p°}\right) = 70 - 2{,}519.\ln\left(\frac{p}{p°}\right) \qquad \text{eq.4}$$

for T=303 K, S° methanol(303K)=240 J.mol^{-1}K^{-1} [36]

Considering that, at the end of the last incremental desorption step, the measured equilibrium pressure value is 1 Torr, the adsorption heat corresponding to the desorbing sites is found to be -87 kJ.mol^{-1}. Note that this value appears quite consistent with the experimental average q^{diff} value taken

from figure 4. From table 3, such a value in the heat of adsorption can be related to the interaction of methanol with all dissociating sites at low coverage, including the less energetic one, S2-IN (-88 kJ.mol^{-1}), but also, from table 4, to the interaction of methanol at higher coverage up to S2-ON-2m (-84 kJ.mol^{-1}) or S2-ON-3m systems. From the energetic values related to the dissociative (S2-ON-3m-*fd*: ~-81 kJ.mol^{-1}) or molecular (S2-ON-3m-*pd*: -89 kJ.mol^{-1}) adsorption of the third molecule, it could be inferred that irreversible adsorption sites are not limited to dissociating sites, but may also involve molecular adsorption sites.

Infra-red spectroscopy appears thus as very complementary to microcalorimetry to solve this point since it allows discriminating between molecular and dissociative adsorptions modes. Two decompositions of the infra-red experimental spectrum obtained after introduction of 1 Torr of methanol were performed on the basis of the three main bands previously reported (molecular and dissociative, L"=1 and L"=2, adsorption modes) in the one hand and following the new assignment involving an additional band relative to L"=3 species. In fact, both decompositions presented on figure 5 lead to similar results: the total amount of methanol adsorbed for P_{eq} =1 Torr is found to be 6.5 µmol.m^{-2}, including 1.5 µmol.m^{-2} for dissociative adsorption modes and 5 µmol.m^{-2} for molecular adsorption. In fact, the L"=3 species, taken into account in figure 5b, weakly impacts the quantification. This can raise from two main reasons : (i) the absorption coefficients strongly differs from molecular to dissociated species[28] and (ii) the population of sites that are responsible for the additional L"=3 contribution (kinks and divacancies) is expected to be relatively low, as evidenced by microcalorimetry measurements. In fact, this result confirms that the semi quantitative classification on deprotonation abilities of MgO samples of various morphologies toward methanol[13,19] performed on the basis of Bensitel assignments[10] are still valid.

The surface density of irreversible adsorption sites obtained by microcalorimetry is directly comparable with the total amount of methanol adsorbed measured by infra-red (7 and 6.5 µmol.m^{2}, respectively). Thus, from a volumetric method on one hand and a spectroscopic one on the other hand, very consistent quantitative data are obtained thanks to similar pretreatment procedures applied for both

techniques. These data are also in the same range than quantifications obtained by various other methods for MgO samples of various morphologies, as shown in table 5: whereas annealed (100) single crystal does not irreversibly adsorb any methanol, all defective samples, from sputtered single crystal to high surface powders, with different pretreament conditions, adsorbed from 5 to 8 μmol.m^{-2}. Thus, strong adsorption takes place on surface defects and the similar quantitative results reported in table 5 tend to show that the amount of strongly adsorbed methanol does not depend on MgO morphologies.

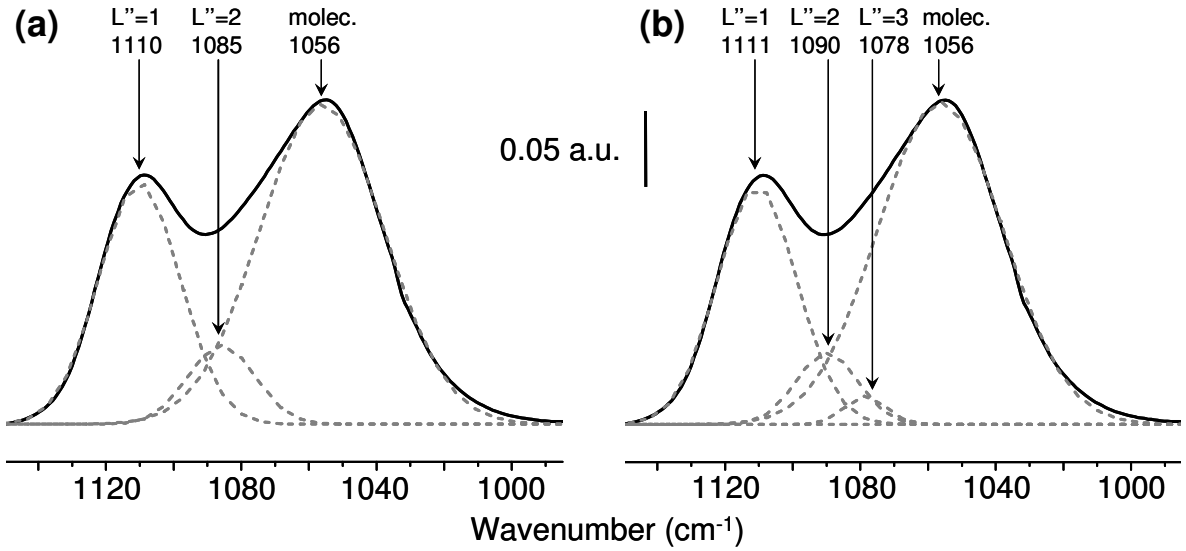

Figure 5: Decompositions of the experimental infra-red spectrum of MgO sol gel obtained after introduction of methanol (P_{eq}=1 Torr) at room temperature within three (a) or four bands (b) .

However, it was shown that the catalytic activity[13] as well as the deprotonation abilities[10,19] of MgO powders do depend on morphologies, and both increase with increasing proportion of ions in low coordination.[13] In fact, if the "strongly adsorbed molecules" had long been intuitively assigned to dissociative adsorption,[15] the present study evidences that the link between strength of the adsorbing site and nature of the adsorption mode is not so obvious. Indeed, from quantitative infra-red studies only 25% of the irreversible adsorption concerns dissociation on the MgO sol gel sample. Such discrepancy between the amount of dissociating sites and the total amount of strong sites is explained by theoretical calculations. Indeed, we have clearly evidenced that, among the molecular adsorption sites that were

usually intuitively ascribed to the weak 5C ions basic sites, there do also exist sites as strong as dissociating ones, on defective surfaces at high methanol coverage.

Table 5: Surfacic density of methanol adsorbed at RT on MgO

MgO sample	method	pretreatment before adsorption	conditions for measurement	surface density of adsorbed methanol ($\mu mol.m^{-2}$)	reference
(100) single crystal	XPS	900 K, UHV	After UHV evacuation at 300 K	0	[15]
(100) single crystal	XPS	Ar sputtering	After UHV evacuation at 300 K	6,3	[15]
powders[§]	volumetric isotherm	773 K, vacuum	irreversible adsorption	6 - 7	[42]
powders[§]	^{13}C NMR	773 K, vacuum	immobile species	5 – 6[*]	[42]
powders	gravimetry	1023 K, vacuum	after evacuation at 298 K	5,2 - 7,8	[10]
sol gel powder	microcalorimetry	1173 K, vacuum	irreversible adsorption	7	present work
sol gel powder	infra-red[28]	1173 K, vacuum	after evacuation at 298 K	6.5	present work

* the isotropic peak related "mobile" methanol appears above this value

§ of various morphologies issued from -vacuum decomposition of carbonate, brucite and oxalate[42] - smoke, commercial MgO (Merck), thermal decomposition of brucite or carbonate[10]

5 Conclusion

The interaction of methanol, used as a probe molecule to characterize the Brønsted basicity for the MgO surface has been studied coupling DFT modeling with experimental techniques. Adsorption modes (geometries and vibrational frequencies) and related adsorption energies are calculated in a periodic approach for a large and representative set of models for MgO surface defects, such as steps, corners and kinks. The adsorption geometries, energies and corresponding vibrational $O_{L'C}H$ frequencies are highly consistent with those reported for water adsorption:[20,23] methanol can thus be used to generate and to study $O_{L'C}H$ experimentally when no method can distinguish $O_{L'C}H$ and $O_{L''C}H$ from water deprotonation on MgO.[12] The calculated values are then compared with experimental data obtained by infra-red and microcalorimetry measurements on highly defective MgO powder pretreated in the same conditions in order to evaluate the relationships between nature, strength and amount for the basic sites involved in the deprotonation process. Mixed adsorption modes (molecular and dissociative) are evidenced with modeling and infra-red. At low coverage, molecular adsorption is observed only on

terraces: all defective sites lead to dissociative adsorption mode. However, the relaxation ability of the surface as well as H bonding interactions are greatly influenced by methanol coverage. So the dissociation ability is modified and may finally favor strongly adsorbed molecular species at high coverage. Thus, contrary to what is usually considered, the link adsorption mode and strength of basic site is not straightforward: molecular adsorption mode is not limited to weak basic sites but it also concerns sites as strong as dissociating ones. Beside coverage, the surface topology governs the structure and the stability of the methoxy groups resulting from dissociation. These groups can be mono-, di- or even tri-coordinated to magnesium cations. The latter configuration is the most stabilizing one and is observed on very confined defects (kinks and divacancies). Although never reported before for this system, its occurrence is confirmed by microcalorimetric detection of sites involving very high differential heats of adsorption (with average value of 280 $kJ.mol^{-1}$). More generally, the calculated range of adsorption energies is in very good agreement with the experimental one. The calculation of vibrational frequencies of the various adsorption structures allows us to refine the previous assignment proposed by Bensitel et al.[10] by including the contribution of the new tri-coordinated species. Finally, quantitative assessment of the strongly adsorbing sites is made through two complementary techniques. With microcalorimetry, this density of sites is obtained by following the adsorption-desorption-adsorption cycles and in infra-red, the ν_{CO} domain is integrated by taking into account absorption coefficients. A very good agreement is obtained for irreversible adsorption (~ 6 $\mu mol.m^{-2}$), but only infra-red allows us to go further with the quantitative discrimination between the sites involved in molecular (~ 5 $\mu mol.m^{-2}$) and dissociative (~ 1.5 $\mu mol.m^{-2}$) adsorption, only the latter being involved in basic reactivity. The involvement of such significant amount of strong basic sites leading to molecular adsorption is rationalized by the influence of methanol coverage on the adsorption modes evidenced by DFT modeling.

ACKNOWLEDGMENT

The authors wish to express their gratitude to David Loffreda from the Ecole Normale Superieure de Lyon for very interesting discussions. Most of the calculations were carried out at the CNRS-IDRIS computational centre (Orsay, France), under project number 051847. The authors thank the ANR BASICAT (Project : ANR-05-JCJC-0256-01) and program COST D-41 for financial support.

RFERENCES

(1) Brønsted, J. N. *Rec. Trav. Chim. Pays-Bas* **1923**, *42*, 718.

(2) Aramendia, M. A.; Borau, V.; C.Jimenez; Marinas, A.; Mrinas, J. M.; Urbano, F. J. *J. Catal* **2002**, *211*, 556.

(3) Uvarova, E. B.; LM Kustov, L. M.; Kazanski, V. B. *Stud. Surf. Sci.* **1995**, *94*, 254.

(4) Thomasson, P.; Tyagi, O.; Knozinger. *Appl Catal A gen* **1999**, *181*, 181.

(5) Ivanov, A. V.; Koklin, A. E.; Uvarova, E. B.; Kustov, L. M. *Phys. Chem. Chem. Phys* **2003**, *5*, 4718.

(6) Bailly, M.-L.; Costentin, G.; Krafft, J. M.; Che, M. *Catalysis Letters* **2004**, *92*, 101.

(7) Mordenti, D.; Grotz, P.; Knozinger, H. *Catal Today* **2001**, *70*, 83.

(8) Lavalley, J.; Lamotte, J.; Travert, J.; Csyniewska; Ziolek, M. *J Chem Soc Farad trans* **1998**, *94*, 331.

(9) Montagne, X.; Lynch, J.; Freund, E.; Lamotte, J.; Lavalley, J. C. *J. Chem. Soc. Faraday Trans 1* **1987**, *83*, 1417.

(10) Bensitel, M.; Saur, O.; Lavalley, J. C. *Mater. Chem. Phys.* **1991**, *28*, 309.

(11) Di Valentin, C.; Vitto, A. D.; Pacchioni, G.; Abbet, S.; Worz, A. S.; Judai, K.; Heiz, U. *J Phys Chem B* **2002**, *106*, 11961.

(12) Chizallet, C.; Costentin, G.; Lauron-Pernot, H.; Maquet, J.; Che, M. *Appl. Catal. A* **2006**, *307*, 239.

(13) Bailly, M. L.; Chizallet, C.; Costentin, G.; Krafft, J. M.; Lauron-Pernot, H.; Che, M. *J. Catal.* **2005**, *235*, 413.

(14) Chizallet, C.; Bailly, M. L.; Costentin, G.; Lauron-Pernot, H.; Krafft, J. M.; Bazin, P.; Saussey, J.; Che, M. *Catal. Today* **2006**, *116*, 196.

(15) Peng, X. D.; Barteau, M. A. *Langmuir* **1991**, *7*, 1426.

(16) Natal-Santiago, M. A.; Dumesic, J. A. *J. Catal.* **1998**, *175*, 252.

(17) Ruppert, A. M.; Meeldijk, J. D.; Kuipers, B. W. M.; Erne, B. H.; Weckhuysen, B. M. *Chem.A Eur. J.* **2008**, *14*, 2016.

(18) Zhang, W.; Wang, H.; Wei, W.; Sun, Y. *J. Mol. Catal. A* **2005**, *231*, 83.

(19) Chizallet, C.; Bailly, M. L.; Costentin, G.; Lauron-Pernot, H.; Krafft, J. M.; Bazin, P.; Saussey, J.; Che, M. *Catalysis Today* **2006**, *116*, 196.

(20) Chizallet, C.; Costentin, G.; Che, M.; Delbecq, F.; Sautet, P. *J.Phys.Chem. B* **2006**, *110*, 15878.

(21) Chizallet, C.; Costentin, G.; Lauron-Pernot, H.; Krafft, J. M.; Che, M.; Delbecq, F.; Sautet, P. *J. Phys. Chem. C* **2008**, *112*, 16629.

(22) Chizallet, C.; Costentin, G.; Lauron Pernot, H.; Krafft, J. M.; Che, M.; Delbecq, F.; Sautet, P. *J. Phys Chem C* **2008**, *112*, 19710.

(23) Chizallet, C.; Costentin, G.; Che, M.; Delbecq, F.; Sautet, P. *J. Am. Chem. Soc.* **2007**, *129*, 6442.

(24) Chizallet, C.; Costentin, G.; Lauron-Pernot, H.; Che, M.; Bonhomme, C.; Maquet, J.; Delbecq, F.; Sautet, P. *J. Phys. Chem. C* **2007**, *111*, 18279.

(25) Busca, G.; Rossi, P. F.; Lorenzelli, V.; Benaissa, M.; Travert, J.; Lavalley, J. C. *J. Phys. Chem.* **1985**, *89*, 5433.

(26) Rossi, P. F.; Busca, G.; Lorenzelli, V.; Lion, M.; Lavalley, J. C. *J. Catal.* **1988**, *109*, 378.

(27) Rossi, P. F.; Busca, G.; Lorenzelli, V.; Waqif, M.; Saur, O.; Lavalley, J. C. *Langmuir* **1991**, *7*, 2677.

(28) Moulin, B.; Oliviero, L.; Costentin, G.; Lauron-Pernot, H.; Bazin, P.; Maugé, F. *in preparation*.

(29) Perdew, J.; Wang, Y. *Phys. Rev. B* **1992**, *45*, 13244.

(30) Kresse, G.; Hafner, J. *Phys. Rev. B* **1994**, *49*, 14251.
(31) Kresse, G.; Furthmüller, J. *Comput. Mat. Sci.* **1996**, *6*, 15.
(32) Kresse, G.; Joubert, D. *Phys. Rev. B 1* **1999**, *59*, 1758.
(33) Badri, A.; Binet, C.; Lavalley, J. C. *J. Chem. Soc. Faraday Trans* **1997**, *93*, 1159.
(34) Schintke, S.; Messerli, S.; Pivetta, M.; Patthey, F.; Libioulle, L.; Stengel, M.; De Vita, A.; Schneider, W. D. *Phys. Rev. Lett.* **2001**, *87*, 276801.
(35) Fubini, B. *Therrnochim. Acta* **1988**, *135*, 19.
(36) Stull, D. R.; Westrum, E. F.; Sinke, G. C. The chemical thermodynamics of organic compounds; John Wiley and Sons, I., Ed. New York, 1969.
(37) Daturi, M.; Binet, C.; Lavalley, J. C.; Galtayries, A.; Sporken, R. *Phys Chem Chem Phys* **1999**, *1*, 5717.
(38) Frisch et al., M. J. *Gaussian 03, Revision C.02 2004, Gaussian, Inc., Wallingford CT.*
(39) Branda, M. M.; Peralta, J. E.; Castellani, N. J.; Contreras, R. H. *Surf. Sci.* **2002**, *504*, 234.
(40) Gay, I. D.; Harrison, N. M. *Surf. Sci.* **2005**, *591*, 13.
(41) Angenault, J. *Symétrie et Structure, cristallochimie du solide,*Paris, 2001.
(42) Liang, S. H.; Gay, I. D. *Langmuir* **1985**, *1*, 593.